SCATTERING OF SH WAVES BY CRACKS AND DELAMINATIONS IN A CLADDED PLATE

R. L. Bratton and S. K. Datta
Department of Mechanical Engineering and CIRES
University of Colorado
Boulder, CO 80309-0427

A. H. Shah
Department of Civil Engineering
University of Manitoba
Winnipeg, Manitoba Canada R3T 2N2

INTRODUCTION

Recent investigations of space construction have explored the use of Al cladded graphite/epoxy materials for space platforms. Characterization of potential flaws and joints in the cladded material by non-destructive evaluation (NDE) methods ensures the reliability of the structure. One possible NDE method is to use anti-plane shear (SH) waves generated and detected by electromagnetic–acoustic transducers (EMATs). There have been some investigations on the interactions of SH waves with delamination defects in a bimaterial plate. References to some of these can be found in Kundu[1,2]. Scattering of SH waves by cracks in a homogeneous plate was studied by Abduljabbar, et al.[3-5].

In this paper we use the hybrid method described in [3] to analyze SH wave scattering in a cladded anisotropic plate. The hybrid method used here combines a finite element representation in a bounded region of the plate with the modal representation in the exterior region. All the irregularities, e.g., delaminations, matrix cracks, etc., are assumed to be in the bounded region. The cladding material is assumed to be isotropic and the plate to be transversely isotropic with the symmetry axis parallel to the plane of the plate. The problem of scattering by a normal surface-breaking crack in the cladding is studied here. For pure mode SH propagation and scattering it is necessary that the propagation direction be perpendicular to the crack edges and coincides with one of the principle axes of the anisotropic material.

GOVERNING EQUATIONS

The plate being modelled in this paper is shown in Fig. 1 and is assumed to be of uniform thickness H with traction free surfaces. The plate is composed of two materials: an aluminum layer over a fiber-reinforced graphite/epoxy plate. The total thickness of the plate is unity. The thicknesses of the aluminum layer and the graphite/epoxy plate are given in Table 1 as well as the elastic constants. As shown in Fig. 1, all the inclusions or inhomogeneities are contained in the interior region bounded by the vertical boundaries at $x = x_{right}$ and $x = x_{left}$. The incident waves studied here are assumed to be time harmonic SH waves propagating in the $\pm x$ directions of Fig 1. The common factor $\exp(-\imath\omega t)$ is dropped from the remaining expressions. In the domain of the plate the y^{th} component is the only non–vanishing displacement. The total displacement at the boundaries is the sum of the incident

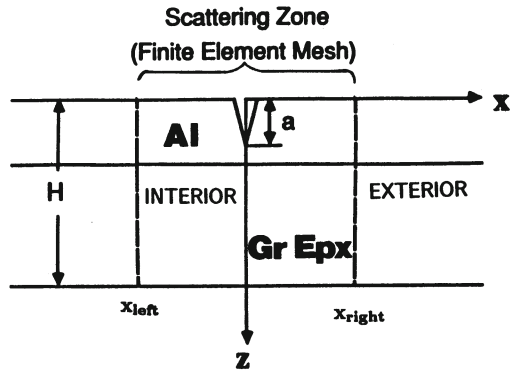

Fig. 1 Geometry of the plate including the crack.

TABLE 1

MATERIAL PROPERTIES				
	C_{44} (N/m^2)	C_{66} (N/m^2)	ρ (g/cm^3)	**Thickness** *(Dimensionless)*
Al	2.413×10^{10}	2.413×10^{10}	2.7	0.35
Gr/Epy	0.350×10^{10}	0.707×10^{10}	1.2	0.65

and scattered displacements,

$$V = V^i + V^s, \tag{1}$$

where V^i denotes the incident field and V^s represents the scattered field.

The incident field is taken as a single shear mode of order m travelling in the positive x direction written in the following form:

$$V^i = A_m V_m(z) e^{ik_m x}. \tag{2}$$

where k_m is the wave number of the incident mode, A_m is the amplitude of the wave and $V_m(z)$ is the mode shape whose largest value is normalized to one. The exterior scattered field is approximated by superposition of a finite number of normal modes. These modes are either propagating or evanescent in the negative and positive x directions, respectively. This can be expressed by the following:

$$V^{s^-}(x,z) = \sum_{n=0}^{N} B_n^- V_n(z) e^{-\imath kx}, \qquad x \le -x_{left} \tag{3a}$$

$$V^{s^+}(x,z) = \sum_{n=0}^{N} B_n^+ V_n(z) e^{\imath kx}, \qquad x \ge x_{right}, \tag{3b}$$

where B_n^+ and B_n^- are undetermined amplitudes of the n^{th} mode of the scattered field. The number of modes necessary to obtain the undetermined amplitudes is equal to the number of nodes on one of the vertical boundaries. Consequently, the number of nodes on each vertical boundary must be the same. These modes are found using the method described in Datta *et al.*[6], where the plate is subdivided into thinner laminae. The displacements distribution within each lamina is expressed in Hermite polynomials preserving continuity of displaements and tractions at the interfaces of adjacent laminae. The accuracy of this method is shown to be excellent [6]. The displacement in the interior region is represented by finite elements. In this paper quarter point and transition elements are employed to describe the crack tip singularity. The variational principle is used to form an impedance matrix $[S] = [K] - \omega^2[M]$ relating the total displacements to the imposed forces at the nodes on the boundaries of the finite element mesh. The impedance matrix can be written in terms of the interior and exterior displacements in the following form,

$$\begin{bmatrix} S_{BB} & S_{IB} \\ S_{BI} & S_{BB} \end{bmatrix} \begin{bmatrix} U_I \\ U_B \end{bmatrix} = \begin{bmatrix} 0 \\ F_B \end{bmatrix}. \tag{4}$$

Condensation of (4) allows U_B, the total displacements on the boundaries, to be determined in terms of the nodal forces of the exterior field,

$$U_B = [S_{BB} - S_{BI} S_{II}^{-1} S_{IB}]^{-1} F_B. \tag{5}$$

The forces F_B are composed of the scattered fields plus the incident field such that

$$F_B = \int \tau_{xy}^{s\pm}\, dz + \int \tau_{xy}^{i}\, dz, \tag{6}$$

where $\tau_{xy}^{s\pm} = C_{66} \partial V^{s\pm}/\partial x$ and $\tau_{xy}^{i} = C_{66} \partial V^{i}/\partial x$. Using the approach in [3], the nodal forces on the left and right boundaries are obtained as,

$$F_B^+ = \Delta h C_{66} \left(\frac{\partial V^{s+}}{\partial x} + \frac{\partial V^{i}}{\partial x} \right) \qquad F_B^- = -\Delta h C_{66} \left(\frac{\partial V^{s-}}{\partial x} + \frac{\partial V^{i}}{\partial x} \right),$$

where the negative sign in F_B^- is necessary for consistent sign convention in the finite element formulation and the area, Δh, over which the stress acts. The final form of the nodal forces for the j^{th} node are,

$$F_{Bj}^- = \sum_{n=0}^{N} -(C_{66}^I \Delta h^I + C_{66}^{I+1} \Delta h^{I+1}) V_{nj} (\imath k_m A_m \delta_{mn} e^{-\imath k_m x_{left}} - \imath k_n B_n^- e^{\imath k_n x_{left}}) \tag{7a}$$

$$F_{Bj}^+ = \sum_{n=0}^{N} (C_{66}^I \Delta h^I + C_{66}^{I+1} \Delta h^{I+1}) V_{nj} \imath k_n (A_m \delta_{mn} + B_n^+ e^{\imath k_n x_{right}}), \tag{7b}$$

where I and I+1 indexes represent the material properties and area above and below the j^{th} node, respectively. The area Δh^I is half of the distance between the I-1 and I node and the area Δh^{I+1} is half of the distance between the I and I+1 node.

From (5) U_B can now be determined by

$$\begin{bmatrix} U_B^- \\ U_B^+ \end{bmatrix} = [S_{BB} - S_{BI}S_{II}^{-1}S_{IB}]^{-1} \begin{bmatrix} F_B^- \\ F_B^+ \end{bmatrix}. \tag{8}$$

Consequently, U_B^- and U_B^+ can now be used to solve for the reflection and transmission coefficients B_n^- and B_n^+, respectively. Using the known values of U_B, the impedance matrix, and the incident field amplitudes A_m, B_n^+ and B_n^- can be found by the algebraic solution of (8). Furthermore, the total interior displacements U_I can be obtained from (4) by

$$U_I = S_{II}^{-1}S_{IB}U_B. \tag{9}$$

This results in the total displacements at the interior nodes for the finite element mesh including the nodes on the crack or inclusion.

DISSCUSION OF RESULTS

Two checks were made to validate the numerical calculations. First, for an incident wave without any inclusion or crack in the interior region, the resulting scattered field is negligible. The reflection coefficients for this case were on the order of 10^{-6}. This demonstrates energy conservation, since no artificial energy sources or sinks are present to distort the reflected and transmitted fields. Second, the reciprocity relation given below in (10) was verified,

$$k_m R_{nm} = k_n R_{mn} \frac{\int C_{66}(z)V_n(z)\,dz}{\int C_{66}(z)V_m(z)\,dz}. \tag{10}$$

In the present section, numerical results are presented for R_{mn}. In the example under consideration the plate was divided into 20 lamina. Thus 21 terms in the Fourier series have been taken. This requires the use of 21 nodes along each of the vertical boundaries of the mesh. The amplitudes of the incident mode is taken as one. Zeroth, first, and second incident modes were considered. The results are presented in terms of the reflection coefficients R_{mm} (the solid lines in Figs 2-4) and the conversion coefficients for the reflected modes $R_{mn}, m < n \leq N_p$ (the broken lines of dots and dashes in Figs. 2-4), where m is the incident mode and N_p is the number of propagating modes. The conversion coefficients greater than the incident mode are shown, since the reflected modes of orders less than m can be computed from the reciprocity relation (10). In Figs 2–4 the variations of R_{mn} with frequency are shown for a crack length, **a**, of 0.2, with a non-dimensional frequency of $\omega H/\sqrt{C_{66}/\rho}$ using graphite/epoxy's constants. The abrupt variations at the critical or cutoff frequencies are due to the inception of new propagating modes, which causes sudden change in the distribution of energy in the spectra of the reflected and transmitted waves. Thus the converted modes n due to an incident mode m cannot exist until the frequency has reached the corresponding cutoff frequency for that converted mode n.

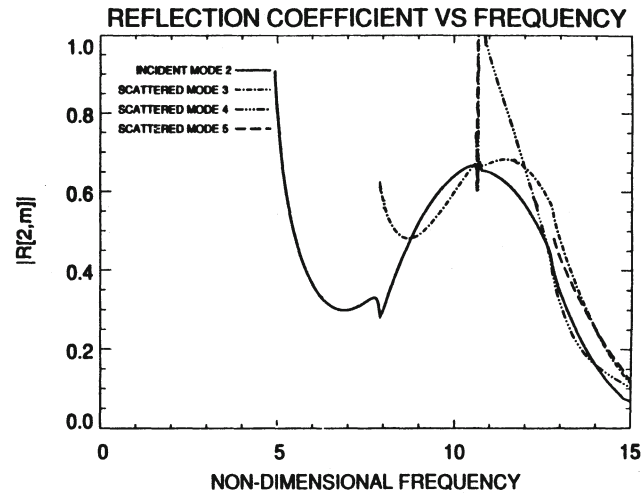

Fig. 2 Magnitude of $|R_{0n}|$ versus non-dimensional frequency.

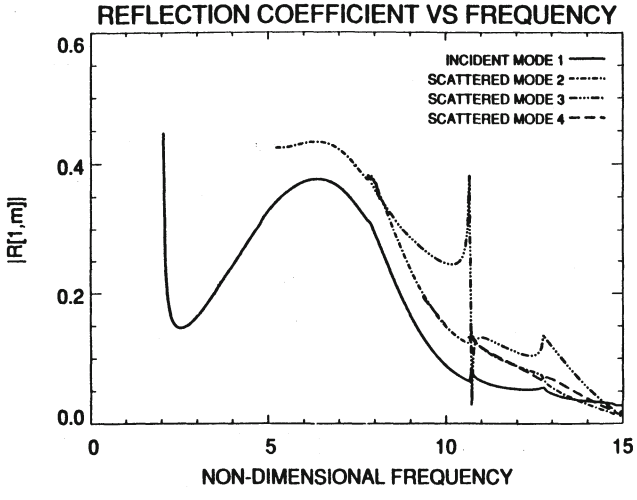

Fig. 3 Magnitude of $|R_{1n}|$ versus non-dimensional frequency.

CONCLUSION

A hybrid method has been presented for studying the diffraction of horizontally polarized shear (SH) waves in plates. The technique replaces a bounded region containing the scatterers by finite elements. This allows such inclusions as slanted surface breaking cracks, buried cavities, and delaminations between two materials to be modelled. Moreover the materials can be isotropic and anisotropic as well as layered. In the exterior regions, the field is written as a modal sum. Continuity conditions at the boundary between the the interior and exterior regions of the plate are then obtained with the aid of the discrete Fourier analysis. Although results presented here are for normal surface–breaking cracks, the method can be used for other defects like, canted and buried cracks, delaminations. These results will be communicated later.

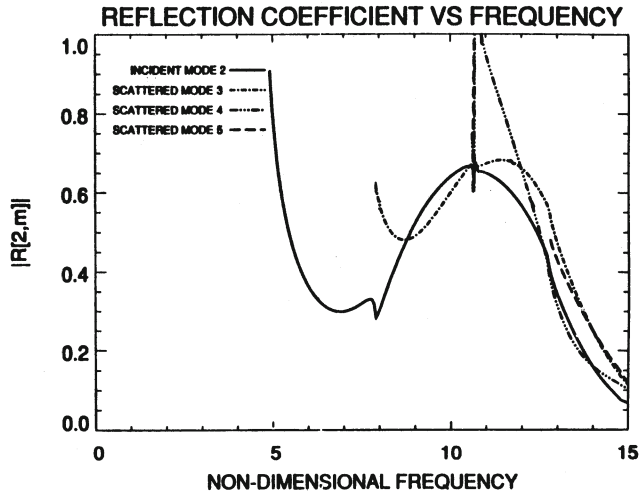

Fig. 4 Magnitude of $|R_{2n}|$ versus non-dimensional frequency.

ACKNOWLEDGEMENT

The work reported here has been supported in part by a grant from the Office of Naval Research (#N00014-86-K-02800), Scientific Officer: Dr. Y. Rajapakse) and by grants from the National Science Foundation (MSM-860913, INT-85214222, and INT-8610487). Support was received also from the Natural Science and Engineering Research Council of Canada (A-7988).

REFERENCES

1. T. Kundu and T. Hassan, Int. J. Fract., 35 55 (1987).
2. T. Kundu, J. Appl. Mech., 53 579 (1986).
3. Z. Abduljabbar ,S. K. Datta and A. H. Shah, J. Appl. Phys. 20, 461 (1983).
4. Z. Abduljabbar and S. K. Datta, in Numerical Methods for Transient and Coupled Problems, R. W. Lewis, E. Hinton, P. Betess, and B. A. Schreffer, eds., Pineridge Press, Swansia (1984).
5. S. K. Datta, R. E. Schramm, and Z. Abduljabbar, in Review of Progess in Qunatitative Nondestructive Evaluation, vol. 6A, D. O. Thompson and D. E. Chimenti, eds., Plenum Press, New York (1987).
6. S. K. Datta, A. H. Shah, R. L. Bratton and T. Chakarborty, J. Acoust. Soc. Am. 83, 2020 (1988).